

# 1 Two decades of land cover mapping in the Río de la Plata 2 grassland region: the MapBiomias Pampa initiative

3 Baeza, S.<sup>1\*</sup>; Vélez-Martin, E.<sup>2</sup>; De Abelleira D.<sup>3</sup>; Banchemo, S.<sup>3</sup>; Gallego, F.<sup>4</sup>; Schirmbeck, J.<sup>2</sup>;  
4 Veron, S.<sup>3, 5</sup>; Vallejos, M.<sup>6</sup>; Weber, E.<sup>7</sup>; Oyarzabal, M.<sup>5</sup>; Barbieri, A.<sup>8</sup>; Petek, M.<sup>3</sup>; Guerra Lara  
5 M.<sup>9</sup>; S. Sarraillhé, S.<sup>3</sup>; Baldi, G.<sup>10</sup>; Bagnato. C.<sup>11</sup>; Bruzzone, L.<sup>4</sup>; Ramos, S.<sup>8</sup>; Hasenack, H.<sup>12</sup>,

6 <sup>1</sup> Departamento de Sistemas Ambientales, Facultad de Agronomía, UdelaR. Montevideo 12900, Montevideo  
7 Uruguay; [sbaeza@fagro.edu.uy](mailto:sbaeza@fagro.edu.uy)

8 <sup>2</sup> GeoKarten Consultoria em Tecnologia da Informação Ltda. Roca Sales 95735-000, Rio Grande do Sul, Brasil;  
9 [evelezmartin@gmail.com](mailto:evelezmartin@gmail.com) , [schirmbeck.j@gmail.com](mailto:schirmbeck.j@gmail.com)

10 <sup>3</sup> Instituto de Clima y Agua, Instituto Nacional de Tecnología Agropecuaria (INTA) Hurlingham 1686, Buenos  
11 Aires, Argentina; [deabelleyra.diego@inta.gob.ar](mailto:deabelleyra.diego@inta.gob.ar) , [banchemo.santiago@inta.gob.ar](mailto:banchemo.santiago@inta.gob.ar) , [veron@agro.uba.ar](mailto:veron@agro.uba.ar) ,  
12 [ssarraillhe@agro.uba.ar](mailto:ssarraillhe@agro.uba.ar) , [mpetek@agro.uba.ar](mailto:mpetek@agro.uba.ar)

13 <sup>4</sup> Instituto de Ecología y Ciencias Ambientales, Facultad de Ciencias, UdelaR. Montevideo 11400, Montevideo  
14 Uruguay; [fgallego@fcien.edu.uy](mailto:fgallego@fcien.edu.uy) , [lolibruzzone@gmail.com](mailto:lolibruzzone@gmail.com)

15 <sup>5</sup> Departamento de Métodos Cuantitativos y Sistemas de Información, LART, IFEVA, Facultad de Agronomía,  
16 UBA/CONICET. Buenos Aires 1417, Buenos Aires, Argentina; [oyarzabal@agro.uba.ar](mailto:oyarzabal@agro.uba.ar)

17 <sup>6</sup> Programa de Investigación en Producción y Sustentabilidad Ambiental, Instituto Nacional de Investigación  
18 Agropecuaria. El semillero 70006, Colonia, Uruguay; [mvallejos@inia.org.uy](mailto:mvallejos@inia.org.uy)

19 <sup>7</sup> Departamento Interdisciplinar e Programa de Pós-Graduação em Sensoriamento Remoto, Universidade  
20 Federal do Rio Grande do Sul, Campus Litoral Norte. Tramandaí 95590-000, Rio Grande do Sul;  
21 [eliseu.weber@ufrgs.br](mailto:eliseu.weber@ufrgs.br) .

22 <sup>8</sup> Departamento de Geografía, Facultad de Ciencias, UdelaR. Montevideo 11400, Montevideo Uruguay;  
23 [abarbieri@fcien.edu.uy](mailto:abarbieri@fcien.edu.uy) , [sebastianramos897@gmail.com](mailto:sebastianramos897@gmail.com)

24 <sup>9</sup> Instituto de Matemática Aplicada San Luis, Universidad Nacional de San Luis y CONICET. San Luis 5700, San  
25 Luis, Argentina; [guerralara@agro.uba.ar](mailto:guerralara@agro.uba.ar)

26 <sup>10</sup> Instituto de Matemática Aplicada San Luis, Universidad Nacional de San Luis and CONICET. San Luis 5700, San  
27 Luis, Argentina; [baldi@unsl.edu.ar](mailto:baldi@unsl.edu.ar)

28 <sup>11</sup> IRNAD, UNRN, CONICET, San Carlos de Bariloche 8400, Río Negro, Argentina.; [bagnato@agro.uba.ar](mailto:bagnato@agro.uba.ar)

29 <sup>12</sup> Departamento de Ecologia, IB e Programa de Pós-Graduação em Agronegócios, CEPAN, Universidade Federal  
30 do Rio Grande do Sul. Porto Alegre 91501-970, Rio Grande do Sul, Brasil; [hhasenack@ufrgs.br](mailto:hhasenack@ufrgs.br)

31 \* Correspondence: [sbaeza@fagro.edu.uy](mailto:sbaeza@fagro.edu.uy)

## 32 **Abstract**

33 The Río de la Plata Grasslands (RPG) region is the largest area of the temperate humid and sub-humid  
34 grasslands biome in South America and one of the largest in the world. The region is located on  
35 fertile soils, generally very suitable for agricultural development, so it is undergoing an intense land  
36 cover change process. Our knowledge of these changes remains incomplete. Most regional-scale  
37 studies have been conducted over specific periods, limited subsets of the RGP, coarse resolution and,  
38 in general, used land cover classes that are not readily compatible. In this work we described and  
39 analyzed the land cover changes in the entire RPG region for the first two decades of the 21st  
40 century, especially those related to grasslands loss. We generated annual land cover maps with 30-  
41 meter resolution that discriminate between 8 categories: native woody formation, forest plantation,  
42 swampy areas and flooded grassland, grassland, farming, non-vegetated area, water and non-  
43 observed. The map series was evaluated for the years 2001 and 2018 using a completely  
44 independent dataset, selected by stratified randomized sampling. Overall accuracy was 73.5% and

45 77.8% for 2001 and 2018, respectively, with user and producer accuracies that varied between  
46 classes and years. In 20 years, RPG region lost, at least, 2.4 million ha of grassland (9% of the  
47 remaining grassland area in 2001). Most of these losses are concentrated in Brazil and Uruguay and  
48 are associated with new agricultural or forestry areas that increased by 5% and 100%, respectively.  
49 Our maps allow a comprehensive understanding of the transformation processes that RPG are  
50 undergoing and provide the context on which to explore a large set of hypotheses related to  
51 ecosystem structure and functioning. It will also contribute to improving decision-making at both the  
52 regional and national levels.

53 **Keywords:** Land use change, Landsat, Time series, Grasslands, Classification

## 54 **1. Introduction**

55 The disruption of ecosystem structure and functioning is a ubiquitous feature of the  
56 interaction between people and nature and it is generally referred to as land use or land cover  
57 change. An increasing number of studies show that human transformative land cover practices have  
58 impacted on carbon, nitrogen and hydrologic balance, biodiversity and climate (Hansen et al. 2013,  
59 Steffen et al. 2015) across multiple spatio-temporal scales (Ellis et al. 2021). In addition, land cover  
60 changes are triggered by a complex and bundled set of driving forces –from population increase,  
61 social inequality, market forces, infrastructure development, and individual responses to economic  
62 or technological opportunities which are in turn mediated by institutional factors (Lambin et al.  
63 2001)-, which defy simplifications and require local or regional approaches to improve our  
64 understanding and assist decision making.

65 The RPG, also known as "Campos" or "Pampas", is the largest temperate grassland region in  
66 South America and one of the largest in the world, with an area of more than 70 million hectares,  
67 covering the great plain of central-eastern Argentina, Uruguay and the south of Brazil (Soriano,

68 1991). They are renowned for their rich and productive vegetation mainly composed of grasses and  
69 herbs (Andrade et al. 2018; Lezama et al. 2019) and for providing habitat to a diverse and specific  
70 biota, including 109 species of grassland birds (Azpiroz et al. 2012). However, these grasslands are  
71 among the most altered ecoregions of the world as less than 1% of their area is subject to any kind of  
72 use restriction (Henwood 1998, Hoekstra et al. 2005, Watson et al. 2016). Thus, over the last 200  
73 years large tracts of native grasslands have been mainly replaced by sown pastures, crops, and tree  
74 plantations (Baeza & Paruelo, 2018; Hall et al. 1992; Viglizzo et al. 2001). Together with the economic  
75 benefits brought about by the international trade of grain, meat, and other primary goods, public  
76 concerns on the sustainability and conservation of the RPG have intensified (Rotolo et al. 2015). The  
77 expansion of agriculture has significant impact on biodiversity (Staude et al. 2018), biological  
78 invasions (Guido et al. 2016), and carbon (Caride et al. 2012; Guershman et al. 2003), nitrogen  
79 (Austin et al. 2006) and hydrologic cycles (Noseto et al. 2012). The replacement of grasslands by  
80 Eucalyptus plantations have been documented to reduce soil pH, increase evapotranspiration, and  
81 may cause soil salinization (Jobbagy & Jackson, 2003; Nosetto et al. 2005). Moreover, cattle and  
82 sheep grazing have been shown to increase or decrease grasslands aboveground net primary  
83 production (Altesor et al. 2005; Rusch & Oesterheld, 1997) depending on the effects of changing  
84 species, plant functional type composition, biomass, and vertical distribution upon water and  
85 nutrient availability (Altesor et al. 2005).

86 Despite its importance, our understanding of the land cover changes and grassland  
87 conservation status in the RPG remains incomplete, coarse and fragmented. Most regional-scale  
88 studies have focused on the portion of the RPG limited to a given country and generally use official  
89 agricultural statistics aggregated at county level to characterize land cover changes (Baeza et al.  
90 2014, Paruelo et al. 2006, Viglizzo et al. 2011). In turn, detailed studies have been conducted over  
91 specific periods, limited subsets of the RGP, coarse resolution and, in general, used land cover classes  
92 that are not readily compatible (Baeza & Paruelo, 2018, 2020; Baldi et al. 2008; Cordeiro & Hasenack,  
93 2009; Graesser et al. 2015, Souza et al. 2020; Volante et al. 2015). Thus, while these studies have

94 been instrumental to highlight the magnitude of the anthropogenic alteration of the RPG  
95 ecosystems, information on what remains and where, at what rates and over which type of land  
96 cover changes have been actively occurring is still lacking.

97           Our knowledge of the Earth's surface dynamics has increased in pace with remote sensing  
98 technological advances. Compared to conventional ground-based approaches, remote sensing is  
99 particularly advantageous to monitor large areas due to its synoptic and repetitive observations. The  
100 recent advent of Google Earth Engine (GEE) (Gorelick et al. 2017), together with easy access of global  
101 very high-spatial resolution images, the increased availability of digital tools to create and edit  
102 geographical data and crowdsourcing data collection protocols have opened the door for  
103 customized, periodic, and accurate land cover monitoring (Azzari & Lobell 2017). Indeed, the  
104 availability of long term (>20 years) annual time series of land cover maps over national, continental  
105 or global extents produced with an objective and reproducible methodology and consistent legends  
106 represents a giant step forward in our ability to characterize past, and predict future, land cover  
107 changes, its environmental and social impacts and enhance territorial planning (Souza et al. 2020).

108           The MapBiomas initiative (<https://mapbiomas.org>) was created to develop a methodology  
109 capable of generating annual land cover maps based on Landsat satellite imagery collection, in a  
110 concept of progressively evolving land cover map collections. Data is processed using machine  
111 learning algorithms at GEE and both, land cover maps and the algorithms used, are publicly available.  
112 The work is carried out by a network of interdisciplinary teams linked to universities, NGOs,  
113 technology companies and startups, operating in a collaborative environment. It involves  
114 methodological development as well as incorporates local knowledge on land cover to improve  
115 results. Started in Brazil (see Souza et al. 2020), the initiative has recently expanded to map land  
116 cover and its changes over time in different biomes, such as the Gran Chaco Americano  
117 (<https://chaco.mapbiomas.org/>; Banchemo et al. 2020), Pan Amazonia

118 (<https://amazonia.mapbiomas.org/>) or the Atlantic Forest  
119 (<https://bosqueatlantico.mapbiomas.org/es>).

120 Here we describe and analyze the land cover changes that occurred between 2000 and 2019  
121 in the RPG using satellite based annual time series of land cover maps at 30 m resolution. To achieve  
122 this goal, we first developed and implemented a mapping framework – based on Landsat imagery  
123 and a GEE random forest classifier trained with visually interpreted samples- to produce a consistent  
124 land cover maps time series from the RPG biome. We then characterized the spatio-temporal pattern  
125 of land cover in the RPG focusing on the following questions: i) which is the present status of land  
126 cover types and how did they change in the last 20 years, ii) where have the rates of grassland –or  
127 other land cover conversion been highest, and iii) which have been the most frequent land cover  
128 transitions?

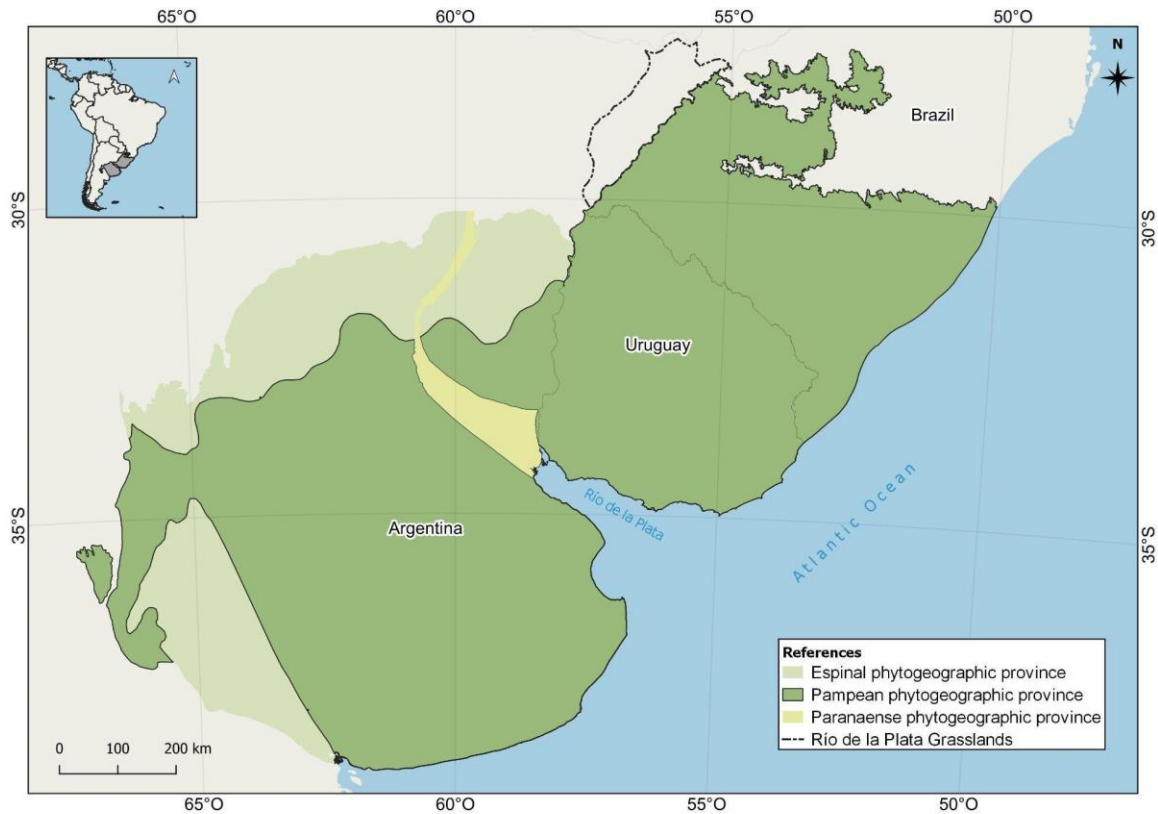
## 129 2 Materials and Methods

### 130 *2.1 Study Area and land cover mapping approach*

131 The RPG occupies ca. 700000 km<sup>2</sup> (28°S–38°S, 50°W–61°W) (Soriano, 1991) and it ranges  
132 over 3 countries, central-eastern Argentina, Uruguay and part of southern Brazil. The mean annual  
133 temperature decreases from 20°C in the north to 13°C in the south, and the annual precipitation  
134 ranges from 1500 mm in the northeast to 400 mm in the southwest (Oyarzabal et al. 2020).  
135 Grasslands, formed by different combinations of C3 and C4 grasses and a broad set of herbs are the  
136 dominant vegetation (Andrade et al. 2018; Soriano 1991).

137 In this work, we focus only on the changes that have occurred within the RPG region.  
138 However, the total area mapped within the scope of the trinational MapBiomas Pampa initiative  
139 includes most of the RPG and also, parts of the neighboring phytogeographic regions of the Espinal  
140 and the Parana delta (Figure 1 ) to keep internal spatial continuity in the maps and with other

141 MapBiomass network initiatives. Results for the entire area covered by MapBiomass Pampa Collection  
142 1 can be found on the project website (<https://pampa.mapbiomas.org/>).

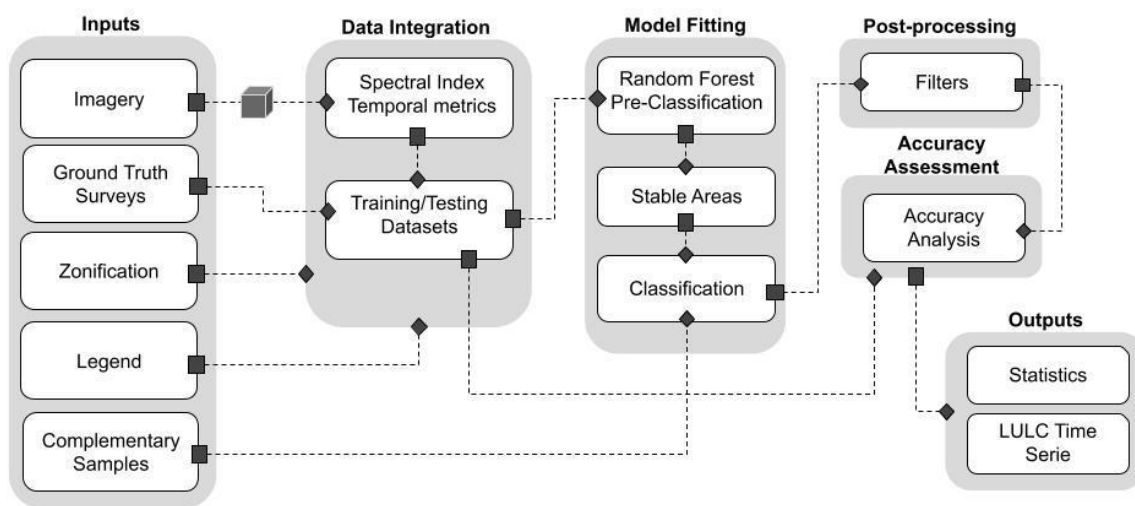


143

144 Figure 1: Region of interest mapped in the MapBiomass Pampa initiative, including the typical areas of  
145 the Pampa, Espinal, and Paraná river Delta.

146 The workflow of the classification process of Collection 1 in the MapBiomass Pampa initiative  
147 is shown in Figure 2. Having the study area defined, a legend with nine classes, a zonification of the  
148 area, with the definition of homogeneous sub-regions, and annual Landsat mosaics were generated.  
149 Visual interpretation samples for each class were obtained within each zone. The samples were  
150 generated using spectral data, vegetation indices and their temporal metrics. These were divided  
151 into training samples and testing samples and used only to perform a pre-classification with the  
152 random forest algorithm. From the pre-classification maps, then a new set of training stable samples  
153 (i.e. samples obtained from sites with the same class along the study period) was established and

154 used as a basis for the final classification using the random forest algorithm again. To improve the  
 155 classification within each sub-region, a set of complementary training stable samples was collected  
 156 *ad hoc* and through visual interpretation. The post-processing of the classification consisted of a set  
 157 of spatial, temporal and frequency filters. The results of this methodology were annual maps of the  
 158 study area together with statistics regarding area and annual land cover transitions. The  
 159 classifications were validated through a review process for the years 2001 and 2018, with a set of  
 160 independent samples.



161  
 162 Figure 2: Workflow implemented for the classification process of Collection 1 of the MapBiomias  
 163 Pampa initiative.

164 **2.2 Inputs**

165 **2.2.1 Zonification**

166 The classification process was carried out in 23 homogeneous sub-regions, nine in Argentina,  
 167 seven in Brazil and seven in Uruguay (Figure S1, Supplementary material). These units correspond to  
 168 relatively homogeneous areas established to perform the classifications independently, avoiding the  
 169 use of samples from other sub-regions. Thus, each subregion is a geographical classification unit.



170 Zonification was based on different sources of information depending on each country: in Argentina,  
171 were included vegetation indices, cropland, rivers and water bodies density maps and climate  
172 information. In Uruguay, zonification was based on geomorphology criteria (Panario et al. 2014) and  
173 in Brazil, through a combination of soils, geomorphology and vegetation (Hasenack 2017).

174

### 175 2.2.2 Imagery

176 The imagery dataset used was obtained from the Landsat sensors Thematic Mapper (TM),  
177 Enhanced Thematic Mapper Plus (ETM+) and the Operational Land Imager and Thermal Infrared  
178 Sensor (OLI-TIRS), on board of Landsat 5, Landsat 7 and Landsat 8, respectively. The Landsat imagery  
179 collections with 30 m pixel resolution were accessible via Google Earth Engine, and were provided by  
180 National Aeronautics and Space Administration (NASA) and United States Geological Survey (USGS).  
181 The imagery dataset used had Tier 1 from USGS and surface reflectance (SR), also had radiometric  
182 calibration and orthorectification correction based on ground control points and digital elevation  
183 model to account for pixel co-registration and correction of displacement errors. For the selection of  
184 Landsat scenes a threshold of 90% of cloud cover was applied (i.e., any available scene with up to  
185 90% of cloud cover was accepted). This limit was established based on a visual analysis, after many  
186 trials observing the results of the cloud removing/masking algorithm.

187 Selected Landsat scenes were merged and clipped within standardized cells for data  
188 processing, hereafter called 'charts', based on the grid of the World International Chart to the  
189 Millionth, at the 1:250,000 scale level. Each chart sets the geographical limits ( $2^{\circ} \times 1.5^{\circ}$  size) to build  
190 up the temporal and spatial Landsat annual mosaics. These mosaics were generated by the  
191 composition of pixels in each set of images, based on the median pixel value over a given period (a  
192 growing season or a year). These medians are constructed with all valid pixels, i.e.: without error  
193 (e.g.: data gaps on Landsat 7 SLC-off images) or cloud masked values. The periods of the year in  
194 which the images were selected varied by country and resulted from the balance between the

195 probability of maximizing the differences in classes' spectral behavior and the availability of cloud-  
196 free images. In Uruguay and Brazil, the considered period was from September to November of each  
197 year while in Argentina from May to July. The three-months periods were extended for some years  
198 and charts when the availability of cloud-free images was low. To proceed with digital classification,  
199 all charts from the same year were merged and clipped by the boundary of the corresponding sub-  
200 region.

### 201 2.2.3 Legend

202 The legend of the MapBiomias Pampa initiative included nine land cover classes (see Table  
203 S1-Supplementary material for a detailed description of each class): native woody formation, forest  
204 plantation, swampy areas and flooded grassland, grassland, farming, non-vegetated area, water, and  
205 non-observed. Native woody vegetation can be divided only in Argentina into two classes, closed  
206 forest and open forest. To maintain internal consistency, this division is not taken into account in this  
207 work and the maps and statistics reported reflect what happened with the entire native woody  
208 vegetation class.

### 209 2.2.4 Training data for Pre-Classification

210 Training samples of each class were obtained by visual interpretation of images and time  
211 series of vegetation indices. For this, backdrops of false-color Landsat mosaics for all the 20 years as  
212 well as graphs showing the temporal behavior of spectral indices per pixel were used to create stable  
213 land cover class samples (i.e. areas where the class was the same during the 20-year period). The  
214 sampling was done drawing small polygons (less than 200 pixels) using GEE Code Editor. On average,  
215 10 polygons per chart and per class were digitized. A total of 4,189 polygons were digitized for  
216 Argentina and 1,703 for Uruguay. These samples were used for the pre-classification process. In the  
217 Brazilian portion there was no sample collection once the pre-classification process followed an  
218 alternative approach (see below).

## 219 2.3 Data integration

220 Landsat imagery was used to generate the feature space (i.e. variables) used as input of the  
221 random forest classifier. For each chart we calculated different aggregation metrics to reduce all  
222 observations within the selected period and produce temporal annual mosaics. Each mosaic has  
223 spectral bands and index, fractions and index from spectral mixture analysis, temporal index (based  
224 on median, minimum, amplitude and standard deviation reducers), and textural index. Each year was  
225 divided into quartiles by the Normalized Difference Vegetation Index values to define the higher and  
226 lower periods of photosynthetic activity. The median values of the highest quartile were defined as  
227 the high activity image and the lowest ones as the low activity image. This criterion was applied over  
228 spectral bands and indices to generate the high and low version of the descriptor (Table S2-  
229 Supplementary material). We obtained a total of 107 bands that allow us to describe the temporal  
230 and spectral dynamics between 2000 and 2019.

231 Training samples were used to generate the training and calibration sets to fit a random  
232 forest classifier. We extracted the values from the mosaics and shuffled the samples following a  
233 holdout strategy, with 70% and 30% to train and validate respectively.

## 234 2.4 Model fitting

### 235 2.4.1 Pre-classification

236 A subset between 200 and 700 pixels per class and per zone were randomly selected from  
237 the pixels of the on-screen-digitized polygons (randomly selected too) and used as training areas for  
238 the classification algorithm. Classification was performed zone by zone, year by year, using the Smile  
239 Random Forest algorithm (Breiman, 2001) available in Google Earth Engine, running 40 iterations  
240 (random forest trees) with 4 variables per split and minimum leaf size of 25. For Argentina and  
241 Uruguay, a total of 20 yearly preliminary classifications were obtained and the frequency with which  
242 a pixel was classified to the same land cover class was calculated to define the temporal stable areas.

243 In Brazil, an existing classification for these 20 years (results of MapBiomass Brazil collection 4.1,  
244 launched in 2019) was used to define the temporal stable areas for each class, making it unnecessary  
245 to produce a pre-classification. The first map collections for this specific region were made using  
246 decision trees based on Spectral Mixture Modeling (MME) variables as is described in Souza Jr. et al.  
247 (2005).

#### 248 2.4.2 Stable areas samples

249 Each pixel classified with the same land cover class for at least a minimum number of years in  
250 the period 2000-2019 is considered as stable. The frequency thresholds depend on the class and the  
251 subregion (e. g. forest plantations for pulp mills usually have a 12-year cycle in Uruguay and a 18-year  
252 cycle in Argentina). The layer of stable areas was generated by those thresholds from which pixels  
253 were extracted for the classification (2,000 samples for each subregion). The selection was random  
254 and stratified based on the class cover percentage. The data set was balanced, rare classes that did  
255 not reach a land cover of at least 10% of the region area had a minimum of 200 samples. The data set  
256 was divided in two categories, training and testing. 60% of the subset, labeled as training pixels, were  
257 used as training samples for the classification algorithm.

#### 258 2.4.3 Complementary data

259 The need for complementary training samples was evaluated by visual inspection comparing  
260 the output of the preliminary classification with both Landsat and high-resolution (< 1m) images  
261 available as base maps in GEE (typically WorldView, GeoEyes or Ikonos imagery) . Complementary  
262 samples were obtained by checking the false-color composites of the Landsat mosaics for all the 20  
263 years during the polygon drawing to ensure class stability. Complementary samples were a minority  
264 (1.4 % of the total samples) and were used in some categories to solve specific classification  
265 problems. For example, wet lowlands grasslands classified as agricultural areas or confusion between  
266 Forest plantations and native woody vegetation in hilly areas, etc.

#### 267 2.4.4 Classification

268 The final classification was performed for all subregions and years with stable and  
269 complementary samples with the algorithm used in the pre-classification (Random Forest, with 40  
270 trees, 4 variables per split and minimum leaf size of 25). All years used the same subset of samples,  
271 but trained using the specific mosaic of the year being classified.

#### 272 2.5 Post-processing

273 The results of the final classification were improved through a sequence of filters, to correct  
274 missing data, “salt-and-pepper” classification errors and, specially, cases of misclassification.

275 The “gap” filter was applied to fill the no-data pixels. The no-data values are replaced by the  
276 temporally nearest valid classification. In this procedure, if no “future” valid position was available,  
277 then the no-data value was replaced by its previous valid class. Therefore, gaps should only exist if a  
278 given pixel has been permanently classified as no-data throughout the entire temporal domain.

279 The spatial filter avoids unwanted modifications to the edges of the pixel groups, a spatial  
280 filter was built based on the "connectedPixelCount" function. Native to the GEE platform, this  
281 function locates connected components (neighbors) that share the same pixel value. Thus, only pixels  
282 that did not share connections to a predefined number of identical neighbors were considered  
283 isolated. In this filter, at least six connected pixels were needed to reach the minimum connection  
284 value. Consequently, the minimum mapping unit is directly affected by the spatial filter applied, and  
285 it was defined as 6 pixels (~0,5 ha).

286 The temporal filter uses the information from the previous year and the later year to identify  
287 and correct a pixel misclassification, considered as cases of invalid transitions. In the first step, the  
288 filter looks at any natural cover (3, 4, 11, 12, 33) that is not this class in 2000 and was kept unchanged  
289 in 2001 and 2002 and then corrects the 2000's value to avoid any regeneration in the first year. In  
290 the second step, the filter looks at a pixel value in 2019 that is not 14 (Farming) but is equal to 14 in  
291 2017 and 2018. The value in 2019 is then converted to 14 to avoid any regeneration in the last year.

292 The third process looks in a 3-year moving window to correct any value that changed in the middle  
293 year and returns to the same class next year.

294 To correct classification problems associated with some classes in specific regions, frequency  
295 filters were applied to use the temporal information available for each pixel to correct cases of false  
296 positives. The general logic of the frequency filter is to search for each pixel a specific combination of  
297 classes throughout the 20 years producing a subset of pixels considered eligible for correction. Then  
298 the filter detects and overwrites only those years where cases of false positives are present using a  
299 fixed class value, that usually is the mode of classifications detected along the temporal range.

## 300 *2.6 Accuracy assessment*

301 We used an independent validation dataset to assess the accuracy of our land cover maps.  
302 To avoid temporal filter effects at the beginning and end of the study period (see above) we selected  
303 for the accuracy analysis the years 2001 and 2018. We followed the sampling scheme proposed by  
304 Olofsson et al. (2014) whereas 2,330 pixels were selected by means of a stratified random design.  
305 Thus, the common accuracy assessment sample consisted of seven strata (one per class) based on  
306 the 2010 land cover map for the entire area covered by MapBiomass Pampa Collection 1. The  
307 allocation of samples to each stratum was slightly shifted from proportional as we fixed a minimum  
308 and maximum number of samples for the rarest and for the most frequent classes. Each of the 2330  
309 samples was evaluated by at least 2 different interpreters (and a third evaluation was required when  
310 initial interpretations disagreed) involving up to 16 interpreters from 3 countries. Interpreters could  
311 access an RGB visualization of a Landsat composite from 2001 and from 2018, a NDVI time-series  
312 plot, and the catalog of very high-resolution images available in Google Earth Pro.

313 Accuracy assessment was performed by comparing the land cover maps with the  
314 independent reference points and calculating non-normalized and normalized error matrices  
315 (Congalton 1991, 2009). From them, we computed a set of commonly used accuracy measures,  
316 comprising producer's and user's accuracy, omission and commission errors, and overall accuracy.

317 Additionally, we computed quantity disagreement (QD) and allocation disagreement (AD), which  
318 decompose the overall disagreement in its components of quantity and allocation (Pontius and  
319 Millones, 2011).

320 These measures were preferred instead of kappa taking into account criticisms about the  
321 meaning and usefulness of the latter in the literature (Foody, 2020; Olofsson et al. 2014; Pontius &  
322 Millones 2011; Stehman et al. 2021). While kappa measures how much the agreement is better than  
323 random, quantity disagreement and allocation disagreement measure how much the agreement is  
324 less than perfect, providing additional information that helps to explain the error. Allocation  
325 disagreement and quantity disagreement provide measures of discordance due to the imperfect  
326 spatial allocation of class pixels and due to the incorrect extent of classes, respectively. Quantity  
327 disagreement measures the amount of difference between the reference data and the classification  
328 map that is due to the less than perfect match in the proportions of the categories. Allocation  
329 disagreement measures the amount of difference between the reference map and the estimated  
330 map that is due to the less-than-optimal match in the spatial allocation of the categories, given the  
331 proportions of the categories in the reference data and in the classification (Pontius & Millones  
332 2011).

### 333 *2.7 Outputs*

334 The area for each class in the annual maps was calculated from the number of pixels. The  
335 statistics were made for different spatial units: biomes, countries, and, in the website, for provinces  
336 and districts. Also, land cover changes occurring in a given period were calculated. In the same way  
337 as in the accuracy analysis, land cover transition for each pixel was calculated for 2001 and 2018, in  
338 order to avoid temporal filter effects. This data is available as spreadsheets, maps and Sankey  
339 diagrams respectively, in the MapBiomias Pampa web-platform. All GEE codes used in the  
340 classification process are available on GitHub [https://github.com/schirmbeckj/mapbiomas-pampa-](https://github.com/schirmbeckj/mapbiomas-pampa-trinacional)  
341 [trinacional](https://github.com/schirmbeckj/mapbiomas-pampa-trinacional)).

342

### 343 3 Results

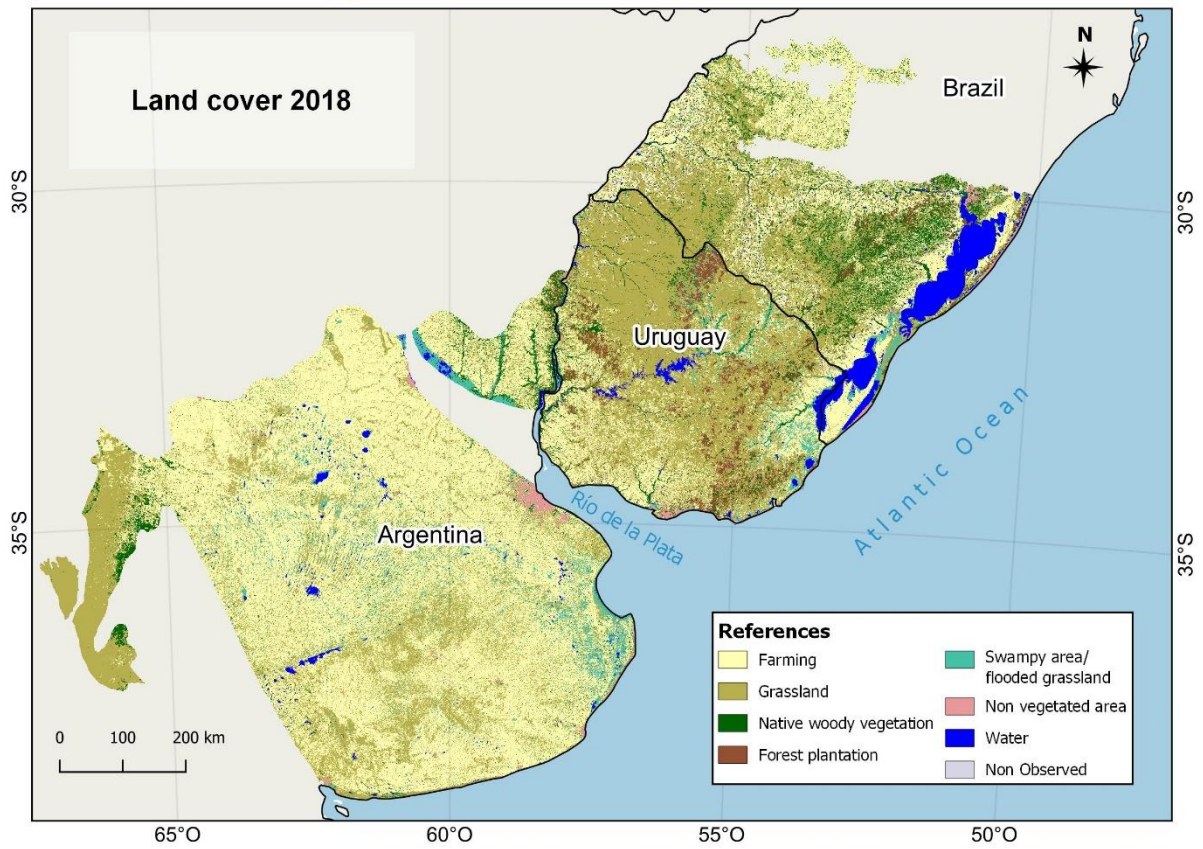
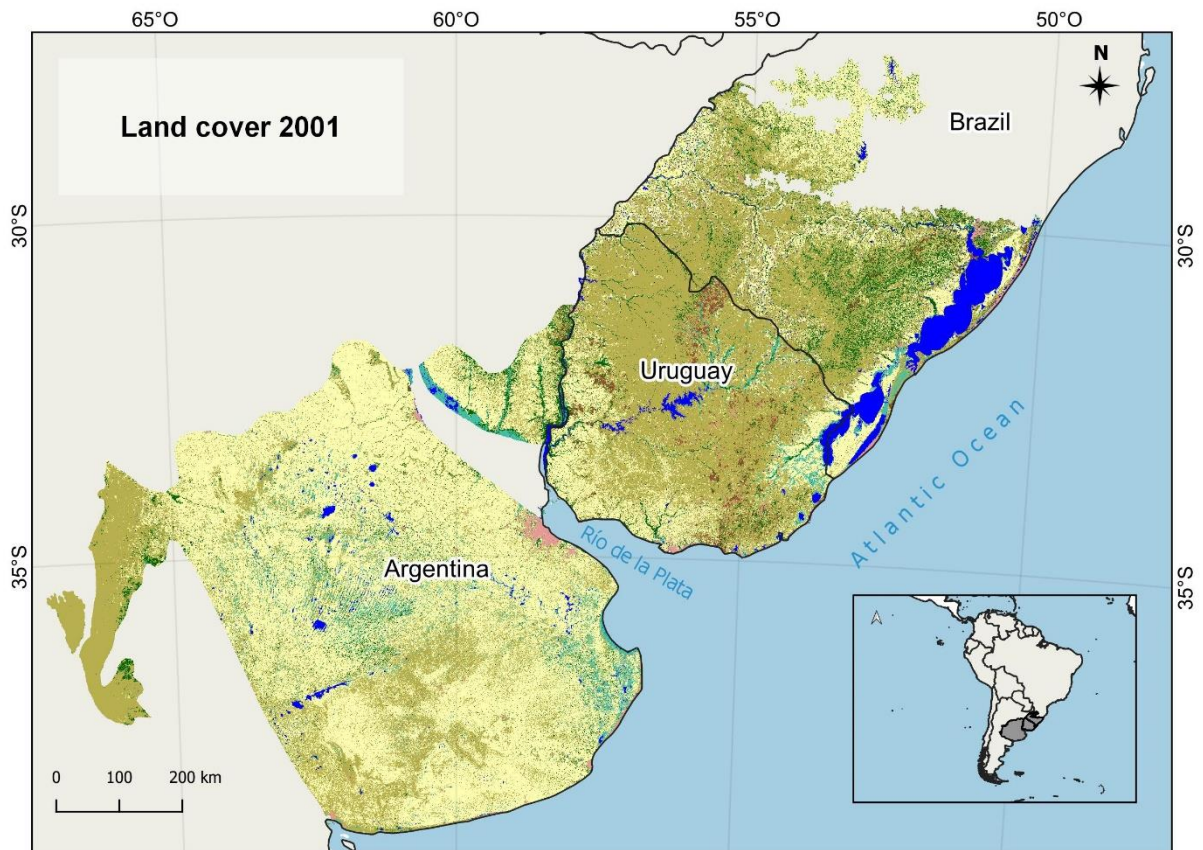
344 Farming and grassland were the most abundant land cover classes in 2001 and 2018 for the  
345 whole region. Native woody vegetation was the third more abundant class, and swampy and flooded  
346 grassland the fourth one. The rest of the classes were relatively scarce (Figures 3 and 4). This general  
347 pattern integrated different individual patterns at country level in 2001 and 2018. In Argentina,  
348 farming was three times more abundant than grassland (Figures 3 and 4). In contrast, in Uruguay,  
349 grassland was three times more abundant than farming (Figures 3 and 4). In Brazil, farming and  
350 grassland were equally abundant, and native woody vegetation was more abundant than in  
351 Argentina and Uruguay (Figures 3 and 4).

352 Forest plantation class relatively increased 100% for the whole region between 2001 and  
353 2018, while farming increased 5% and grassland and native woody vegetation decreased 8-9%  
354 (Figure 4). These general relative changes between 2001 and 2018 integrated different individual  
355 changes at country level. In Argentina, native forest decreased 30%, while forest plantation and  
356 swampy and flooded grassland decreased 7% (Figure 4). In Brazil, forest plantation increased 200%,  
357 farming 25% and native forest 5%, while grassland decreased 25% and swampy and flooded  
358 grassland 3% (Figure 4). In Uruguay, forest plantation increased 100%, swampy and flooded grassland  
359 12% and farming 3%, while grassland area decreased 10% (Figure 4).

360 For the whole region the net loss of grassland was approximately 2.4 million hectares (Mha).  
361 This change includes the loss of 6.2 Mha (21% relative to grassland area in 2001), mainly due to  
362 replacement with farming, and the gain of 4.5 Mha of new grassland areas, mostly from farming. The  
363 transitions between the other classes were smaller and involved less than 0.9 Mha (Figure 5). At  
364 country level, Argentina has a net gain of grassland of 0.3 Mha, resulting for the transition from  
365 grassland to farming (2.8 Mha), from farming to grassland (2.7 Mha) and, to a lesser extent, from  
366 native woody vegetation and swampy area/flooded vegetation to grassland. Loss of native woody



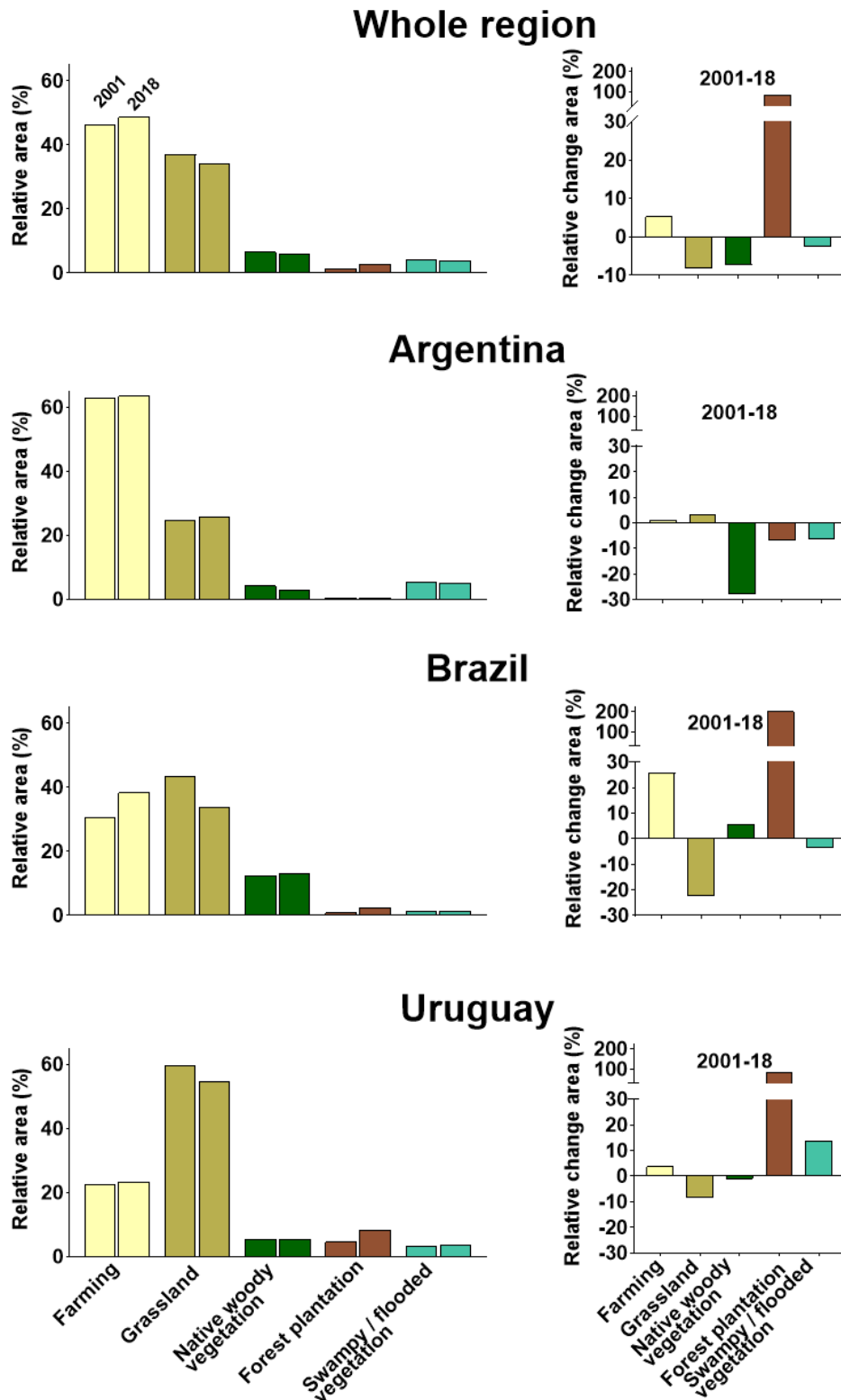
367 vegetation was around 0.6 Mha mainly for conversion to farming. In Brazil, net grassland loss was 1.9  
368 Mha resulting for the transition from grassland to farming (2.1 Mha) and native woody vegetation  
369 (0.4 Mha) and the transition from farming to grassland (0.6 Mha). Uruguay has a net grassland loss of  
370 0.9 Mha resulting for the transition from grassland to farming (1.4 Mha) and forest plantation (0.6  
371 Mha) and the transition from farming to grassland (1.1 Mha). The rest of the transitions were less  
372 important and involved, all together, the change of category of 0.4, 0.2 and 0.2 Mha in Argentina,  
373 Brazil and Uruguay, respectively (Figure 5).



374

375

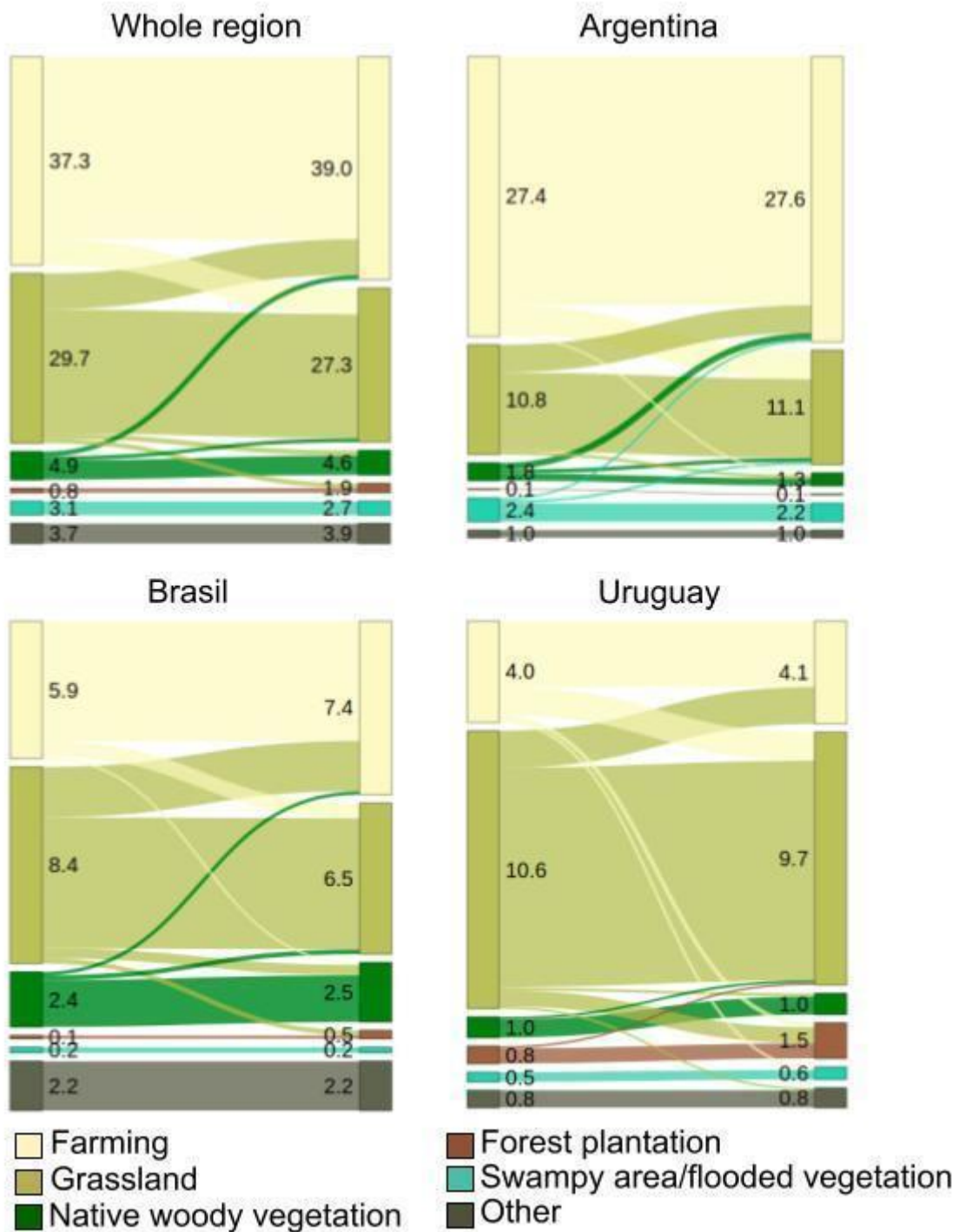
376 Figure 3: Land cover map for Rio de la Plata Grasslands during 2001 (top) and 2018 (bottom). Black  
 377 lines indicate international boundaries.



378

379 Figure 4: Relative area (%) of land cover main vegetated classes for the whole RPG region and each  
 380 country between 2001 and 2018 (left), and relative change area (%; right). Relative change area was  
 381 calculated as:  $(\text{area 2018} - \text{area 2001}) / \text{area 2001}$ . For better readability, only two labels are shown in  
 382 the first top left graphic.

383



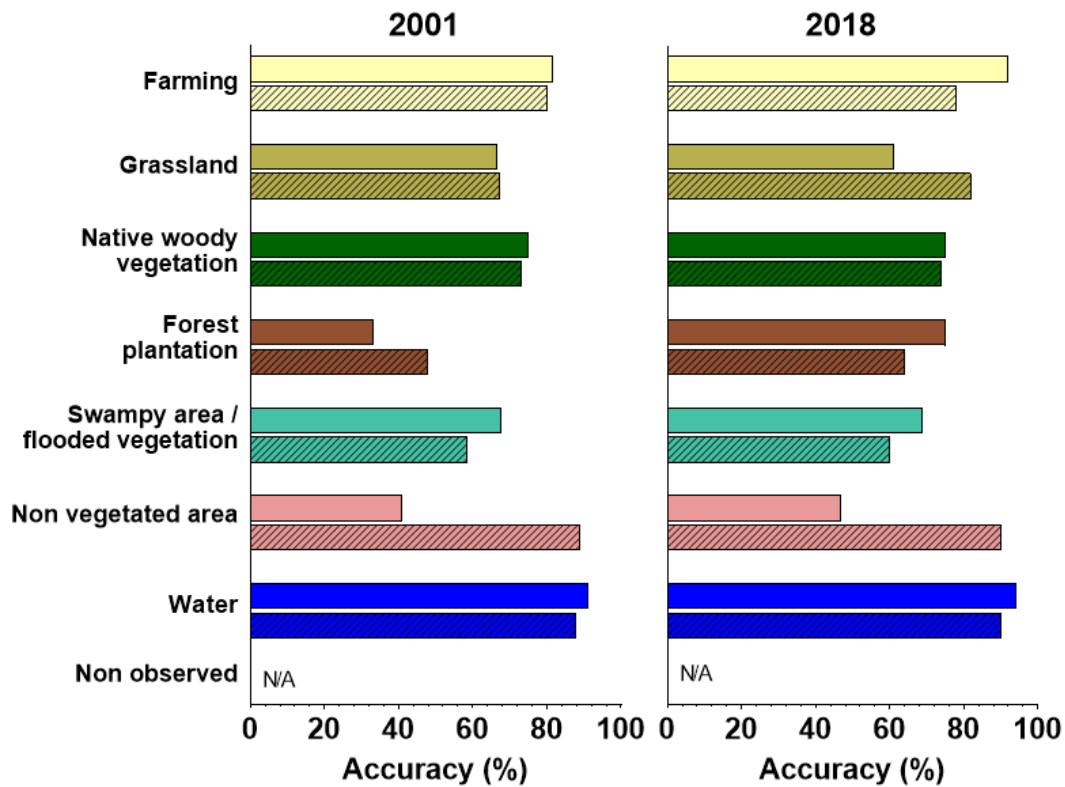
384

385 Figure 5: Transitions of land cover classes for the whole RPG region and each country between  
386 2001 (left) and 2018 (right). Transitions with less than 0.5% of the total area were removed for visual  
387 purposes. In each panel, numbers indicate the area of each class (in million ha).

### 388 *3.1 Accuracy Assessment*

389 Overall accuracy (OA) was 74% for 2001 and 78% for 2018. In 2001, user and producer's  
390 accuracies were maximum for farming and water, and minimum for forest plantations. In 2018, both  
391 accuracies were also maximum for farming and water, user's accuracy was minimum for non-  
392 vegetated area while producer's one was minimum for swampy area/flooded vegetation (Figure 6).  
393 Regarding the nature of disagreements, in both land cover maps, allocation disagreement (AD) was  
394 the major component of discordance with 24.3% in 2001 and 13.1% in 2018. Quantity disagreement  
395 (QD) in 2001 was 2.3% and in 2018, 1.31% (Table S3, Supplementary material). Summing overall  
396 agreement and allocation disagreement gives an indicator of area agreement which equals 97.7% in  
397 2001 and 90.9% in 2018.

398



399  
 400 Figure 6: User's (empty bars) and producer's (scratched) accuracy of land cover maps in 2001 and  
 401 2018.

#### 402 4 Discussion

403 Our work reports land cover and its changes over time for the entire RPG region with  
 404 unprecedented spatial and temporal resolutions (20 years of 30 m annual maps). The MapBiomass  
 405 Pampa initiative summarizes the collaborative effort of three countries and several public and private  
 406 institutions incorporating local knowledge in the construction of maps. RPG region has lost at least 8  
 407 % of its natural grassland area in the last 20 years mainly due to farming and forest plantation  
 408 expansion. These losses were greatest in the Brazilian portion of the study area, where grasslands  
 409 lost almost 30% of their area. Wall to wall (entire region) maps allow a global understanding of the  
 410 transformation processes that RPG are undergoing and provide the context in which to explore a  
 411 large set of hypotheses related to the distribution of plant and animal species, effects of habitat loss

412 and fragmentation on biodiversity, biological invasions or ecosystem functioning. Moreover, our  
413 maps can help to define cooperation on supranational management policies (e.g. planning of road  
414 infrastructure for cargo transport, estimating the final volume of raw materials in different ports,  
415 etc.) or to assess the effect of different land management policies at the national level.

416 Our maps presented accuracies comparable to those reported in other works that map land  
417 cover over large areas and reflect the complexity of mapping natural grasslands. For example,  
418 Buchorn et al. (2020), for Copernicus Global Land Cover - Collection 2, reported a global accuracy  
419 around 80%, accuracies around 70% for herbaceous vegetation and 50-60 % for wetlands and  
420 shrublands. Stheman et al. (2021), reported somewhat higher precision for the annual map series of  
421 the U.S. Geological Survey Land Change Monitoring, with an average overall accuracy of 82.5% but  
422 highly variable in space; for example, the grass/shrub class had user accuracies of 36 and 48% and  
423 producer accuracies of 15 and 11% for east and central-east regions, respectively. Wickham et al.  
424 (2021) analyzed the accuracy of the National Land Cover Database, a Landsat based land cover maps  
425 for the conterminous US, and reported global accuracies of around 72% and user and producer  
426 accuracies of 65 and 67% for grasslands, respectively. The accuracy of our maps was also similar to  
427 that of other map collections from the MapBiomias initiative. For example, Souza et al. (2020) for  
428 annual land cover maps of MapBiomias Brazil - Collection 3, reported overall accuracies ranging from  
429 95 to 73%, depending on the biome considered, with high omission and commission errors for  
430 grassland class. In the Brazilian Cerrado, a particularly complex biome subjected to an intense  
431 process of land cover change, Alencar et al. (2020) mapped native vegetation with overall accuracies  
432 from 67 to 74% and higher errors in grasslands. For MapBiomias Chaco initiative, Banchemo et al.  
433 (2020) reported overall accuracies around 74% but do not report the error distribution of the  
434 different mapped classes. In a direct antecedent that mapped RPG biome, Baeza and Paruelo (2020)  
435 used information on vegetation phenology derived from NDVI-MODIS time series to generate annual  
436 maps for the period 2000-2014. This work had higher accuracy (around 95% at regional level) but  
437 lower conceptual resolution (grouped natural grasslands with sown pastures and native forests with

438 commercial afforestation), lower spatial resolution (250 m) and covered a shorter period of time  
439 than MapBiomass Pampa Collection 1 maps.

440 The accuracy analysis shows coincidences with other works and particular characteristics of  
441 our study area and the approach used. Overall accuracy (and producer / user accuracies) was higher  
442 in 2018 than in 2001, which is expected given the lower availability of high-resolution imagery at the  
443 beginning of the map series, which generates higher uncertainties in both training and evaluation  
444 sample generation. This trend of increasing accuracy of maps from more recent years was also  
445 reported in other works of MapBiomass initiative (Alencar et al. 2020, Souza et al. 2020).

446 A detailed analysis of the confusion matrices including omission and commission errors,  
447 allocation disagreement (AD) and quantity disagreement (QD), and their partial calculus, allows to  
448 identify the main problems of the maps and to infer which classes tend to have their extent  
449 overestimated or underestimated (Table S3, Supplementary material). One of the biggest challenges  
450 in the context of this work is the discrimination of grasslands from other land covers. Grasslands are  
451 mainly confused with farming, probably with sown pastures (included in farming class). The high  
452 physiognomic similarity and the intra class heterogeneity of the spectral response of both natural  
453 grasslands (different communities, landscape positions, location in the study area) and sown  
454 pastures (different species, sowing dates, pasture age, etc.) generate an overlapping of the spectral  
455 signatures of these coverages, which makes it difficult to discriminate between them. Additionally,  
456 and unlike other temperate grasslands where the herbaceous vegetation dries up or is covered with  
457 snow for part of the year, RPGs have photosynthetically active vegetation throughout the year,  
458 making it difficult to discriminate based on phenology. This difficulty for correctly discriminating  
459 grasslands has been reported before in several works and is reflected in the greater confusion of this  
460 category in the land cover works discussed above. For our study area, Rios et al. (2022) reported this  
461 problem for grasslands in southeastern Uruguay, Souza et al. (2020) for South Brazilian grasslands,  
462 Baeza et al. (2019) and Baeza and Paruelo (2020) for Uruguayan grasslands. Baeza and Paruelo (2020)



463 dealt with this grassland-pasture confusion by merging the classes into a single category of perennial  
464 forage resources. Contrary, in our work, pastures were mapped together with crops in a single  
465 Farming class, leaving natural grasslands, the main natural vegetation formation of the biome, as an  
466 independent class.

#### 467 *4.1 Grassland loss and main Land Use Changes.*

468 In 20 years, RPG region lost almost 2.4 million ha of grassland (9% of the remaining grassland  
469 area in 2001). Most of these losses are concentrated in Brazil and Uruguay and are associated with  
470 new agricultural or forestry areas. Similar trends were previously reported in other works that cover  
471 partially (Baldi & Paruelo; 2008; Cordeiro and Hasenack, 2009; Kuplich et al. 2018; Oliveira et al.  
472 2017; Volante et al. 2015) or totally (Baeza et al. 2020; Graesser et al 2015; Potapov et al. 2021) de  
473 study area. Song et al. (2021) recently reported that most of the expansion of the soybean area in  
474 South America occurred at the expense of grassland areas in the RPGs where the area with this crop  
475 practically doubled in the last 20 years. In Argentina, the area with natural grasslands remained  
476 practically unchanged, probably because most of the sites suitable for agriculture had already been  
477 transformed prior to the period analyzed and/or the new agricultural areas come from areas  
478 previously occupied with sown pastures. Baldi & Paruelo (2008) and Viglizzo et al. (2011) reported  
479 that the agriculturalization process in most of the Argentine pampas predates the year 2000. Baeza  
480 and Paruelo (2020) reported changes from perennial forage resources to crops in the Argentine  
481 pampas after 2000. These changes probably respond to an agricultural intensification process with a  
482 shift from sown pastures or pasture-agriculture rotation to continuous annual crops; both land cover  
483 categories fall into the farming class in our classification scheme, which would explain why our maps  
484 do not capture these changes.

485 Another important land cover change process that has occurred in the last two decades is  
486 the increase of forest plantation, which doubled the area occupied compared to 2001. This increase  
487 was particularly important in Uruguay and Brazil, where the forested area doubled and tripled,

488 respectively. In Uruguay, the expansion of forest plantation is associated with political and economic  
489 incentives and the installation of the cellulose industrial complex (Baeza et al. 2006; Baeza and  
490 Paruelo, 2020; Baldi & Paruelo, 2008; Paruelo et al. 2006). In Brazil, it results from private  
491 investments made by large national and international companies to expand the pulp and paper  
492 supply chain within a framework of strong globalization, centralization of assets and concentration of  
493 industrial production (Benetti 2008). A similar process was documented for Argentina, but was  
494 mainly located in North Entre Ríos and Corrientes provinces (Baldi & Paruelo, 2008), areas not  
495 included in this study.

496           Although the accuracy of the maps is moderate, the analysis of the confusion matrix and the  
497 metrics proposed by Pontius and Millones (2011), shows that most of the error is associated with the  
498 allocation and not to quantity disagreement. This increases the map accuracy for area calculation  
499 (Overall accuracy + Allocation disagreement), reaching 98 and 91 % for 2001 and 2018 respectively,  
500 increasing confidence in the loss of grassland areas reported. Moreover, error-corrected area  
501 estimates (Table S4-Supplementary material) show that these grassland losses are surely even  
502 greater. Grassland area was slightly overestimated in 2001 and strongly overestimated in 2018, so  
503 the net loss is probably much higher than calculated from the maps. The opposite occurs with the  
504 two main grassland replacements; Farming underestimation was lower in 2001 than in 2018, from  
505 which it is reasonable to assume that expansion was larger than shown by the maps. Forest  
506 plantations were slightly overestimated in 2001 and considerably underestimated in 2018, implying  
507 that net gain was quite larger than that reported on the maps.

508           The decrease in grassland area coincides with what happened in other grasslands around the  
509 world (Bond and Parr, 2010; Lark et al. 2015; Neke and Du Plais, 2004; Veldman et al. 2015) and  
510 alerts about the conservation status of this biome, often forgotten in the conservation agenda  
511 (Hoekstra et al. 2005; Overbeck et al. 2007; Silveira et al. 2020; Watson et al. 2016). According to  
512 Oyarzabal et al. (2020) there are 99 protected areas in RPG , which cover between 3.7% and 6.8%

513 of the biome extent, depending on the considered regional limits. Most of these protected areas  
514 have been implemented on public lands of generally low-economic importance, regardless of their  
515 conservation values (Baldi et al. 2017, 2019; Oyarzabal et al 2020). The availability of regional  
516 (semi)natural vegetation maps with good spatial and temporal resolution therefore becomes central  
517 for defining efficient conservation and/or restoration policies (Buisson et al. 2021; IPCC, 2019). Our  
518 maps allow systematically identifying both grassland remnants in highly transformed areas and large  
519 grassland patches within landscapes with low fragmentation suitable for conservation programs.

#### 520 *4.2 Limitations and next steps*

521 There are a number of aspects to consider when interpreting the results of this work,  
522 evaluating the scope of generated maps and improving future map collections. The results presented  
523 in this article do not contemplate the entire study area since the maps of MapBiomias Pampa-  
524 Collection 1 also incorporate portions of other neighbor biomes (see methods). However, the  
525 evaluation of the maps was carried out from a stratified sampling that contemplates the entire  
526 mapped area and not exclusively the RPG. This implies that the error estimation and area correction  
527 presented might be slightly different if the stratification and sampling had been done exclusively  
528 within the RPG limits.

529 Future work will require improvements in class differentiation, conceptual resolution (larger  
530 number of classes) and extension of the time period under study. Discrimination improvements  
531 depend on the class to map. In our region, the grasslands confusion discussed above, fundamentally  
532 with sown pastures, could be partially corrected through several mechanisms: improvements in the  
533 quantity and quality of training data; extension of the feature space; use of the historical map series  
534 to discriminate grasslands sites that were previously other land cover. Recently, Rios et al (2022)  
535 used an agricultural mask (sites that had agriculture in at least one of the last 12 years) to  
536 discriminate grasslands from other herbaceous covers (sown pastures, post-agricultural fields with  
537 different stages of vegetal succession) in the southeastern Uruguay. Another class with which

538 grasslands are confused is native woody vegetation, particularly with open woody / savanna  
539 formations, a frequent confusion in systems with variable density of woody cover (Alencar et al.  
540 2020; Sano et al. 2010). Incorporating, at least for the most recent maps, information that accounts  
541 for vegetation structure, such as radar images (see for example: Heckel et al. 2020; Lopes et al. 2020;  
542 Zhang et al. 2019,) or Lidar technology (Ferraina et al. 2022; Ferreira et al. 2011; Zimbres et al. 2020),  
543 could also improve the discrimination of open woody covers and reduce their mixing with grasslands.

544         The improvements in conceptual resolution fundamentally imply the separation of the  
545 farming class between crops and sown pastures and, within crops, between annual and perennial  
546 crops, expanding the potential uses of generated maps (see below). The extension of the studied  
547 period will allow to improve the description of land cover change processes and the analysis of its  
548 causes and consequences. In the RPGs, for example, much of grassland losses, mainly in the  
549 Argentine portion of the study area, occurred before the year 2000 and are not captured in the map  
550 collection presented here. The extension of the map series up to 1985 from the historical Landsat 5  
551 archive has already been successfully used in other works such as MapBiomias Brazil (Souza et al.  
552 2020) or the Land Change Monitoring Assessment and Projection (LCMAP) in the United States  
553 (Brown et al. 2020; Stehman et al. 2021).

554         Due to time and budget constraints, the evaluation of the map collection accuracy was  
555 carried out exclusively for two years, at the beginning and end of the series. An evaluation of the  
556 entire map collection would allow a correct quantification of the rates of change for the different  
557 classes, with more stable trends, enabling the possibility of correcting erroneous transitions.

#### 558 *4.3 The MapBiomias platform and its potential uses*

559         Wall to wall (entire region) RPG maps allow for a comprehensive view of a number of core  
560 aspects linked to ecosystem structure and functioning. They allow to, for example, assess the  
561 biodiversity conservation status and conservation/restoration priorities; model species distribution

562 and design management strategies based on their habitat requirements; assess the role of habitat  
563 loss and fragmentation in biological diversity and/or exotics invasion processes; analyze exchanges of  
564 matter and energy and their influence on the regional climate; or define supranational management  
565 policies. On the other hand, the results allow the comparison of the land use planning policies of the  
566 three countries involved and the evaluation of their effect on the landscape conformation and its  
567 changes over time. For example, the law for the promotion of forestry activities in Uruguay (law  
568 15939) and the installation of 3 large pulp mills, promoted the expansion of forestry plantations  
569 observed in our maps.

570 Previous products from other MapBiomias initiatives, such as MapBiomias Brazil maps'  
571 collections have been used in numerous works. For example, Rosa et al. (2021) quantified native  
572 forest cover dynamics in the Brazilian Atlantic Forest and related them to restoration programs and  
573 Nunes et al. (2020) analyzed the extension and carbon gains of secondary vegetation in the Brazilian  
574 Amazon. Several works also model the impact of land cover changes on energy flows and water cycle  
575 (dos Santos et al. 2022; Laipelt et al. 2021; Rosan et al. 2021) or animal diversity and distribution  
576 (Camana et al. 2020; Alvarenga et al. 2021, Galan Acedo et al. 2021)

577 MapBiomias Pampa land cover maps are conceived as successive evolving collections where  
578 all the products, methods and tools are freely and publicly available on internet  
579 (<https://pampa.mapbiomas.org/>). We hope that the successive maps collection of MapBiomias  
580 Pampa initiative contribute to the development of knowledge and the improvement of decision-  
581 making at both the regional and national levels

582 **Supplementary Materials:** Figure S1: Region of interest mapped in the MapBiomias Pampa initiative  
583 showing the limits of relatively homogeneous areas used to perform independent classifications,  
584 Table S1: Legend description of the MapBiomias Pampa Collection 1, Table S2: Feature space (107  
585 variables) used in the digital classification of Landsat image mosaics in the MapBiomias Pampa  
586 Collection 1 (2000-2019), Table S3: Contingency matrices between classification results and  
587 independent validation dataset, Table S4: Area estimates corrected from the analysis of the  
588 contingency matrices

589 **Acknowledgements:** We would like to thank all the team involved in the MapBiomias Collections and  
590 particularly to Tasso Azevedo (general coordinator) and Marcos Rosa (technical coordinator) from MapBiomias  
591 for promoting and supporting the entire Pampa Trinational initiative. We gratefully acknowledge the USGS and  
592 NASA for the courtesy of the Landsat images. We are also grateful to Google for providing access to the Google  
593 Earth Engine platform that enables the processing of all data. We also thank Fundación Vida Silvestre Argentina  
594 for operating arrangements. This work has been partially funded by MapBiomias Brasil through Arapyaú  
595 Institute. MapBiomias is supported by a network of funders including Children's Investment Fund Foundation  
596 (CIFF), Climate and Land Use Alliance (CLUA), Global Wildlife Conservation (GWC), Good Energies Foundation,  
597 Gordon & Betty Moore Foundation, Iniciativa Internacional de Clima e Florestas da Noruega (NICFI), Instituto  
598 Arapyaú, Instituto Clima e Sociedade (ICS), Instituto Humanize, OAK Foundation, Quadrature Climate  
599 Foundation (QCF), Walmart Foundation (USA), Wellspring Philanthropic Fund (WPC). This work has been also  
600 partially funded by ANII INNOVAGRO projects FSA\_PI\_2018\_1\_149022 and FSA\_PI\_2018\_1\_148811; CSIC I+D  
601 2020\_358, FMV\_3\_2020\_1\_162279, and FMV\_1\_2021\_1\_167032

## 602 References

603 Alencar, A., Z Shimbo, J., Lenti, F., Marques, C.B., Zimbres, B., Rosa, M., ... & Barroso, M. (2020).  
604 Mapping three decades of changes in the brazilian savanna native vegetation using landsat data  
605 processed in the google earth engine platform. *Remote Sensing*, 12(6), 924.

606 Altesor, A., Oesterheld, M., Leoni, E., Lezama, F., & Rodríguez, C. (2005). Effect of grazing on  
607 community structure and productivity of a Uruguayan grassland. *Plant Ecology*, 179(1), 83-91.

608 Alvarenga, G. C., Chiaverini, L., Cushman, S. A., Dröge, E., Macdonald, D. W., Kantek, D. L. Z., ... &  
609 Kaszta, Ż. (2021). Multi-scale path-level analysis of jaguar habitat use in the Pantanal ecosystem.  
610 *Biological Conservation*, 253, 108900.

611 Andrade, B. O., Marchesi, E., Burkart, S., Setubal, R. B., Lezama, F., Perelman, S., ... & Boldrini, I. I.  
612 (2018). Vascular plant species richness and distribution in the Río de la Plata grasslands. *Botanical*  
613 *Journal of the Linnean Society*, 188(3), 250-256.

614 Austin, A. T., Piñeiro, G., & Gonzalez-Polo, M. (2006). More is less: agricultural impacts on the N cycle  
615 in Argentina. *Biogeochemistry* 79: 45–60.

616 Azpiroz, A. B., Isacch, J. P., Dias, R. A., Di Giacomo, A. S., Fontana, C. S., & Palarea, C. M. (2012).  
617 Ecology and conservation of grassland birds in southeastern South America: a review. *Journal of Field*  
618 *Ornithology*, 83(3), 217-246.

619 Azzari, G. & Lobell, D. B. (2017). Landsat-based classification in the cloud: An opportunity for a  
620 paradigm shift in land cover monitoring. *Remote Sensing of Environment* 202: 64–74.

621 Baeza, S. Baldassini, P., Bagnato, C., Pinto, P., Paruelo, J. M. (2014). Caracterización del uso/cobertura  
622 del suelo en Uruguay a partir de series temporales de imágenes MODIS. *Agrociencia Uruguay*, 18  
623 2:95-105.

624 Baeza S. & Paruelo J. 2018. Spatial and temporal variation of Human Appropriation of Net Primary  
625 Production in the Rio de la Plata Grasslands. *ISPRS Journal of Photogrammetry and Remote Sensing*.  
626 145: 238 – 249

627 Baeza, S., & Paruelo, J. M. (2020). Land use/land cover change (2000–2014) in the Rio de la Plata  
628 grasslands: an analysis based on MODIS NDVI time series. *Remote Sensing*, 12(3), 381.

629 Baeza, S., Paruelo, J. M., & Altesor, A. (2006). Caracterización funcional de la vegetación del Uruguay  
630 mediante el uso de sensores remotos. *Interciencia*, 31(5), 382-388.

631 Baeza S.; Rama G. & Lezama F. 2019. Cartografía de los pastizales en las regiones geomorfológicas de  
632 Uruguay predominantemente ganaderas. Ampliación y actualización. En Altesor A, López-Mársico L y  
633 Paruelo J (Eds.). Bases ecológicas y tecnológicas para el manejo de pastizales II., pp. 27-47

634 Baldi, G., Paruelo, J.M. (2008). Land-Use and Land Cover Dynamics in South American Temperate  
635 Grasslands. *Ecology and Society* 13: 6.

636 Baldi, G., Schauman, S., Texeira, M., Marinaro, S., Martin, O. A., Gandini, P., & Jobbágy, E. G. (2019).  
637 Nature representation in South American protected areas: country contrasts and conservation  
638 priorities. *PeerJ*, 7, e7155.

639 Baldi, G., Texeira, M., Martin, O. A., Grau, H. R., & Jobbágy, E. G. (2017). Opportunities drive the  
640 global distribution of protected areas. *PeerJ*, 5, e2989.

641 Banchemo, S., De Abelleira, D., Veron, S. R., Mosciaro, M. J., Arevalos, F., & Volante, J. N. (2020,  
642 March). Recent Land Use and Land Cover Change Dynamics in the Gran Chaco Americano. In 2020  
643 IEEE Latin American GRSS & ISPRS Remote Sensing Conference (LAGIRS) (pp. 511-514). IEEE.

644 Benetti, M. (2008) Indicadores da formação de uma plataforma exportadora de celulose no Rio  
645 Grande do Sul. *Indicadores Econômicos FEE*, Porto Alegre, v. 35, n. 3, p. 21-28.

646 Bond, W. J., & Parr, C. L. (2010). Beyond the forest edge: ecology, diversity and conservation of the  
647 grassy biomes. *Biological conservation*, 143(10), 2395-2404.

648 Breiman, L. Random Forests. *Machine Learning* 2001, 45, 5–32.

649 Brown, J. F., Tollerud, H. J., Barber, C. P., Zhou, Q., Dwyer, J. L., Vogelmann, J. E., ... & Rover, J. (2020).  
650 Lessons learned implementing an operational continuous United States national land change



651 monitoring capability: The Land Change Monitoring, Assessment, and Projection (LCMAP) approach.  
652 *Remote Sensing of Environment*, 238, 111356.

653 Buchhorn M, Lesiv M, Tsendbazar N E, Herold M, Bertels L and Smets B 2020 Copernicus global land  
654 cover layers-collection 2. *Remote Sensing* 12: 1–14.

655 Buisson, E., Fidelis, A., Overbeck, G. E., Schmidt, I. B., Durigan, G., Young, T. P., ... & Silveira, F. A.  
656 (2021). A research agenda for the restoration of tropical and subtropical grasslands and savannas.  
657 *Restoration Ecology*, 29, e13292..

658 Camana, M., Dala-Corte, R. B., Collar, F. C., & Becker, F. G. (2020). Assessing the legacy of land use  
659 trajectories on stream fish communities of southern Brazil. *Hydrobiologia*, 1-16.

660 Caride, C., Piñeiro, G., & Paruelo, J. M. (2012). How does agricultural management modify ecosystem  
661 services in the argentine Pampas? The effects on soil C dynamics. *Agriculture, ecosystems &*  
662 *environment*, 154, 23-33.

663 Congalton, R. G. (1991). A review of assessing the accuracy of classifications of remotely sensed data.  
664 *Remote sensing of environment*, 37(1), 35-46.

665 Congalton, R. G. (2009). Accuracy and error analysis of global and local maps: Lessons learned and  
666 future considerations. *Remote Sensing of Global Croplands for Food Security*, 441, 47-55.

667 Cordeiro, J. L. P., & Hasenack, H. 2009. Cobertura vegetal atual do Rio Grande do Sul. Em: Pillar, V.  
668 D.; Müller, S. C.; Castilhos, Z. M. S. & Jacques, A. V. A. [Eds.]. Campos Sulinos—conservação e uso  
669 sustentável da biodiversidade. Brasília: Ministério do Meio Ambiente, Brasil, 285-299.

670 dos Santos, V. J., Calijuri, M. L., & de Assis, L. C. (2022). Land cover changes implications in energy  
671 flow and water cycle in São Francisco Basin, Brazil, over the past 7 decades. *Environmental Earth*  
672 *Sciences*, 81(3), 1-24.

673 Ellis, E. C., Gauthier, N., Goldewijk, K. K., Bird, R. B., Boivin, N., Díaz, S., ... & Watson, J. E. (2021).  
674 People have shaped most of terrestrial nature for at least 12,000 years. *Proceedings of the National*  
675 *Academy of Sciences*, 118(17).

676 Ferraina, A., Baldi, G., de Abelleira, D., Grosfeld, J., & Verón, S. (2022). An insight into the patterns  
677 and controls of the structure of South American Chaco woodlands. *Land Degradation &*  
678 *Development*, 33( 5), 723– 738.

679 Ferreira, L. G., Urban, T. J., Neuenschawander, A., & De Araújo, F. M. (2011). Use of orbital LIDAR in  
680 the Brazilian Cerrado Biome: Potential applications and data availability. *Remote Sensing*, 3(10),  
681 2187-2206.

682 Foody, G. M. (2020). Explaining the unsuitability of the kappa coefficient in the assessment and  
683 comparison of the accuracy of thematic maps obtained by image classification. *Remote Sensing of*  
684 *Environment*, 239, 111630.

685 Galán-Acedo, C., Spaan, D., Bicca-Marques, J. C., de Azevedo, R. B., Villalobos, F., & Rosete-Vergés, F.  
686 (2021). Regional deforestation drives the impact of forest cover and matrix quality on primate  
687 species richness. *Biological Conservation*, 263, 109338.

688 Graesser, J.; Aide, T. M.; Grau, H. R. & Ramankutty, N. 2015. Cropland/pastureland dynamics and the  
689 slowdown of deforestation in Latin America. *Environmental Research Letters*, 10(3), 034017

690 Gorelick, N., Hancher, M., Dixon, M., Ilyushchenko, S., Thau, D., Moore, R. (2017). Google Earth  
691 Engine: Planetary-scale geospatial analysis for everyone. *Remote Sensing of Environment* 202: 18-27

692 Guerschman, J. P., Paruelo, J. M., & Burke, I. C. (2003). Land use impacts on the normalized  
693 difference vegetation index in temperate Argentina. *Ecological applications*, 13(3), 616-628.

694 Guido, A., Vélez-Martin, E., Overbeck, G. E., & Pillar, V. D. (2016). Landscape structure and climate  
695 affect plant invasion in subtropical grasslands. *Applied Vegetation Science*, 19(4), 600-610.

696 Hall, A.J., Rebella, C.M., Ghersa, C.M., Culot, J.P. Field crop systems of the Pampas. In *Field Crop*  
697 *Ecosystems*; Pearson, C.J., Ed.; Elsevier: Amsterdam, The Netherlands, 1992; pp. 413–450.

698 Hansen, M. C., Potapov, P. V., Moore, R., Hancher, M., Turubanova, S. A., Tyukavina, A., ... &  
699 Townshend, J. (2013). High-resolution global maps of 21st-century forest cover  
700 change. *science*, 342(6160), 850-853.

701 Hasenack, H. Determinantes biofísicos e geopolíticos do uso da terra no estado do Rio Grande do Sul,  
702 Brasil. 2017. 70 f. Tese (Doutorado) - Universidade Federal do Rio Grande do Sul, Centro de Estudos e  
703 Pesquisas em Agronegócios, Programa de Pós-Graduação em Agronegócios, Porto Alegre, BR-RS.

704 Heckel, K., Urban, M., Schratz, P., Mahecha, M. D., & Schullius, C. (2020). Predicting forest cover in  
705 distinct ecosystems: The potential of multi-source Sentinel-1 and-2 data fusion. *Remote Sensing*,  
706 *12*(2), 302.

707 Henwood, W. D. (1998). An overview of protected areas in the temperate grasslands biome. *Parks*,  
708 *8*(3), 3-8.

709 Hoekstra, J.M.; Boucher, T.M.; Ricketts, T.H. & Roberts, C. 2005. Confronting a biome crisis: global  
710 disparities of habitat loss and protection. *Ecology letters*, *8*, 23-29.

711 IPCC, 2019: Climate Change and Land: an IPCC special report on climate change, desertification, land  
712 degradation, sustainable land management, food security, and greenhouse gas fluxes in terrestrial  
713 ecosystems [P.R. Shukla, J. Skea, E. Calvo Buendia, V. Masson-Delmotte, H.-O. Pörtner, D. C. Roberts,  
714 P. Zhai, R. Slade, S. Connors, R. van Diemen, M. Ferrat, E. Haughey, S. Luz, S. Neogi, M. Pathak, J.  
715 Petzold, J. Portugal Pereira, P. Vyas, E. Huntley, K. Kissick, M. Belkacemi, J. Malley, (eds.)]. In press.

716 Jobbágy, E. G., & Jackson, R. B. (2003). Patterns and mechanisms of soil acidification in the  
717 conversion of grasslands to forests. *Biogeochemistry*, *64*(2), 205-229.

718 Kuplich, T. M., Capoane, V.; Costa, L. F. F. O avanço da soja no bioma Pampa. *Boletim Geográfico do*  
719 *Rio Grande do Sul, Porto Alegre, n. 31, p. 83-100, jun. 2018*

720 Lark, T. J., Salmon, J. M., & Gibbs, H. K. (2015). Cropland expansion outpaces agricultural and biofuel  
721 policies in the United States. *Environmental Research Letters, 10(4), 044003.*

722 Lambin, E. F., Turner, B. L., Geist, H. J., Agbola, S. B., Angelsen, A., Bruce, J. W., ... & Xu, J. (2001).  
723 The causes of land-use and land-cover change: moving beyond the myths. *Global environmental*  
724 *change, 11(4), 261-269.*

725 Laipelt, L., Kayser, R. H. B., Fleischmann, A. S., Ruhoff, A., Bastiaanssen, W., Erickson, T. A., &  
726 Melton, F. (2021). Long-term monitoring of evapotranspiration using the SEBAL algorithm and Google  
727 Earth Engine cloud computing. *ISPRS Journal of Photogrammetry and Remote Sensing, 178, 81-96.*

728 Lezama, F., Pereira, M., Altesor, A., & Paruelo, J. M. (2019). Grasslands of Uruguay: classification  
729 based on vegetation plots. *Phytocoenologia, 211-229.*

730 Lopes, M., Frison, P. L., Durant, S. M., Schulte to Bühne, H., Ipavec, A., Lapeyre, V., & Pettorelli, N.  
731 (2020). Combining optical and radar satellite image time series to map natural vegetation: savannas  
732 as an example. *Remote Sensing in Ecology and Conservation, 6(3), 316-326.*

733 Neke, K. S., & Du Plessis, M. A. (2004). The threat of transformation: quantifying the vulnerability of  
734 grasslands in South Africa. *Conservation Biology, 18(2), 466-477.*

735 Noretto, M. D., Jobbágy, E. G., Brizuela, A. B., & Jackson, R. B. (2012). The hydrologic consequences  
736 of land cover change in central Argentina. *Agriculture, Ecosystems & Environment, 154, 2-11.*

737 Noretto, M. D., Jobbágy, E. G., & Paruelo, J. M. (2005). Land-use change and water losses: the case of  
738 grassland afforestation across a soil textural gradient in central Argentina. *Global Change Biology,*  
739 *11(7), 1101-1117.*

740 Nunes, S., Oliveira, L., Siqueira, J., Morton, D. C., & Souza, C. M. (2020). Unmasking secondary  
741 vegetation dynamics in the Brazilian Amazon. *Environmental Research Letters*, 15(3), 034057.

742 Oliveira, T. E. D.; Freitas, D. S. D.; Gianezini, m.; Ruviaro, C. F.; Zago, D.; Mércio, t. Z.; Dias, E. A.;  
743 Lampert, V. D. N.; barcellos, J. O. J. Agricultural land use change in the Brazilian Pampa Biome: The  
744 reduction of natural grasslands. *Land Use Policy*, v. 63, p. 394-400, 2017/04/01/ 2017.

745 Olofsson, P., Foody, G. M., Herold, M., Stehman, S. V., Woodcock, C. E., & Wulder, M. A. (2014). Good  
746 practices for estimating area and assessing accuracy of land change. *Remote sensing of Environment*,  
747 148, 42-57.

748 Overbeck, G. E., Müller, S. C., Fidelis, A., Pfadenhauer, J., Pillar, V. D., Blanco, C. C., ... & Forneck, E. D.  
749 (2007). Brazil's neglected biome: the South Brazilian Campos. *Perspectives in Plant Ecology, Evolution*  
750 *and Systematics*, 9(2), 101-116.

751 Oyarzabal M, Andrade B, Pillar VD, Paruelo JM. 2020. Temperate subhumid grasslands of southern  
752 South America. Pp 1-17. In: Di Paolo, D. Encyclopedia of the World's Biomes. Elsevier, Países Bajos.  
753 ISBN 978-0-12-816096-1.

754 Panario, D., Gutiérrez, O., Sánchez Bettucci, L., Peel, E., Oyhantçabal, P., & Rabassa, J. (2014). Ancient  
755 landscapes of Uruguay. In *Gondwana landscapes in southern South America* (pp. 161-199). Springer,  
756 Dordrecht.

757 Paruelo, J. M., Guerschman, J. P., Piñeiro, G., Jobbagy, E. G., Verón, S. R., Baldi, G., & Baeza, S. (2006).  
758 Cambios en el uso de la tierra en Argentina y Uruguay: marcos conceptuales para su análisis.  
759 *Agrociencia*, 10, 47-61.

760 Pontius Jr, R. G., & Millones, M. (2011). Death to Kappa: birth of quantity disagreement and  
761 allocation disagreement for accuracy assessment. *International Journal of Remote Sensing*, 32(15),  
762 4407-4429.

763 Potapov, P., Turubanova, S., Hansen, M. C., Tyukavina, A., Zalles, V., Khan, A., ... & Cortez, J. (2021).  
764 Global maps of cropland extent and change show accelerated cropland expansion in the twenty-first  
765 century. *Nature Food*, 1-10.

766 Rios, C., Lezama, F. Rama, G., Baldi, G. & Baeza, S. (2022). Natural grassland remnants in dynamic  
767 agricultural landscapes: identifying drivers of fragmentation. *Perspectives in Ecology and*  
768 *conservations*. <https://doi.org/10.1016/j.pecon.2022.04.003>

769 Rotolo, D., Hicks, D., & Martin, B. R. (2015). What is an emerging technology?. *Research policy*,  
770 44(10), 1827-1843.

771 Rosa, M. R., Brancalion, P. H., Crouzeilles, R., Tambosi, L. R., Piffer, P. R., Lenti, F. E., ... & Metzger, J.  
772 P. (2021). Hidden destruction of older forests threatens Brazil's Atlantic Forest and challenges  
773 restoration programs. *Science advances*, 7(4), eabc4547.

774 Rosan, T. M., Goldewijk, K. K., Ganzenmüller, R., O'Sullivan, M., Pongratz, J., Mercado, L. M., ... &  
775 Sitch, S. (2021). A multi-data assessment of land use and land cover emissions from Brazil during  
776 2000–2019. *Environmental Research Letters*, 16(7), 074004.

777 Rusch, G. M., & Oesterheld, M. (1997). Relationship between productivity, and species and functional  
778 group diversity in grazed and non-grazed Pampas grassland. *Oikos*, 519-526.

779 Sano, E. E., Rosa, R., Brito, J. L., & Ferreira, L. G. (2010). Land cover mapping of the tropical savanna  
780 region in Brazil. *Environmental monitoring and assessment*, 166(1), 113-124.

781 Silveira, F. A., Arruda, A. J., Bond, W., Durigan, G., Fidelis, A., Kirkman, K., ... & Buisson, E. (2020).  
782 Myth-busting tropical grassy biome restoration. *Restoration Ecology*, 28(5), 1067-1073.

783 Song, X. P., Hansen, M. C., Potapov, P., Adusei, B., Pickering, J., Adami, M., ... & Tyukavina, A. (2021).  
784 Massive soybean expansion in South America since 2000 and implications for conservation. *Nature*  
785 *sustainability*, 4(9), 784-792.

786 Soriano, A. Rio de la Plata Grasslands. In *Natural Grasslands*; Coupland, R.T., Ed.; Elsevier:  
787 Amsterdam, The Netherlands, 1991; pp. 367–407.

788 Souza, C.M., Jr., Z. Shimbo, J., Rosa, M.R., Parente, L.L., A. Alencar, A., Rudorff, B.F.T., Hasenack, H.,  
789 Matsumoto, M., G. Ferreira, L., Souza-Filho, P.W.M., de Oliveira, S.W., Rocha, W.F., Fonseca, A.V.,  
790 Marques, C.B., Diniz, C.G., Costa, D., Monteiro, D., Rosa, E.R., Vélez-Martin, E., Weber, E.J., Lenti,  
791 F.E.B., Paternost, F.F., Pareyn, F.G.C., Siqueira, J.V., Viera, J.L., Neto, L.C.F., Saraiva, M.M., Sales, M.H.,  
792 Salgado, M.P.G., Vasconcelos, R., Galano, S., Mesquita, V.V., Azevedo, T. Reconstructing Three  
793 Decades of Land Use and Land Cover Changes in Brazilian Biomes with Landsat Archive and Earth  
794 Engine. *Remote Sensing* 2020: 12, 2735

795 Souza, C.M., Jr.; Roberts, D.A.; Cochrane, M.A. Combining spectral and spatial information to map  
796 canopy damage from selective logging and forest fires. *Remote Sensing of Environment*. 2005, 98,  
797 329–343.

798 Staude, I. R., Vélez-Martin, E., Andrade, B. O., Podgaiski, L. R., Boldrini, I. I., Mendonca Jr, M., ... &  
799 Overbeck, G. E. (2018). Local biodiversity erosion in south Brazilian grasslands under moderate levels  
800 of landscape habitat loss. *Journal of Applied Ecology*, 55(3), 1241-1251.

801 Steffen, W., Richardson, K., Rockström, J., Cornell, S. E., Fetzer, I., Bennett, E. M., ... & Sörlin, S.  
802 (2015). Planetary boundaries: Guiding human development on a changing planet. *Science*, 347(6223).

803 Stehman, S. V., Pengra, B. W., Horton, J. A., & Wellington, D. F. (2021). Validation of the US  
804 Geological Survey's Land Change Monitoring, Assessment and Projection (LCMAP) Collection 1.0  
805 annual land cover products 1985–2017. *Remote Sensing of Environment*, 265, 112646.

806 Veldman, J. W., Overbeck, G. E., Negreiros, D., Mahy, G., Le Stradic, S., Fernandes, G. W., ... & Bond,  
807 W. J. (2015). Where tree planting and forest expansion are bad for biodiversity and ecosystem  
808 services. *BioScience*, 65(10), 1011-1018.

809 Viglizzo, E. F., F. Lértora, A. J. Pordomingo, J. N. Bernardos, Z. E. Roberto, and H. Del Valle. 2001.  
810 Ecological lessons and applications from one century of low external-input farming in the pampas of  
811 Argentina. *Agriculture, Ecosystems and Environment*, 83: 65-81.

812 Viglizzo, E. F., Frank, F. C., Carreño, L. V., Jobbagy, E. G., Pereyra, H., Clatt, J., ... & Ricard, M. F. (2011).  
813 Ecological and environmental footprint of 50 years of agricultural expansion in Argentina. *Global*  
814 *change biology*, 17(2), 959-973.

815 Volante, J., Mosciaro, J., Morales Poclava, M., Vale, L., Castrillo, S., Sawchik, J., ... & Paruelo, J. (2015).  
816 Expansión agrícola en Argentina, Bolivia, Paraguay, Uruguay y Chile entre 2000-2010: Caracterización  
817 espacial mediante series temporales de índices de vegetación. *RIA. Revista de investigaciones*  
818 *agropecuarias*, 41(2), 179-191.

819 Watson, J. E., Jones, K. R., Fuller, R. A., Marco, M. D., Segan, D. B., Butchart, S. H., ... & Venter, O.  
820 (2016). Persistent disparities between recent rates of habitat conversion and protection and  
821 implications for future global conservation targets. *Conservation Letters*, 9(6), 413-421.

822 Wickham, J., Stehman, S. V., Sorenson, D. G., Gass, L., & Dewitz, J. A. (2021). Thematic accuracy  
823 assessment of the NLCD 2016 land cover for the conterminous United States. *Remote Sensing of*  
824 *Environment*, 257, 112357.

825 Zhang, W., Brandt, M., Wang, Q., Prishchepov, A. V., Tucker, C. J., Li, Y., ... & Fensholt, R. (2019). From  
826 woody cover to woody canopies: How Sentinel-1 and Sentinel-2 data advance the mapping of woody  
827 plants in savannas. *Remote Sensing of Environment*, 234, 111465.

828 Zimbres, B., Shimbo, J., Bustamante, M., Levick, S., Miranda, S., Roitman, I., ... & Alencar, A. (2020).  
829 Savanna vegetation structure in the Brazilian Cerrado allows for the accurate estimation of  
830 aboveground biomass using terrestrial laser scanning. *Forest Ecology and Management*, 458, 117798.